Structure and up-conversion luminescence of Pr^{3+}/Yb^{3+} co-doped $CaNb_2O_6$ thin films by pulsed laser deposition

Yinzhen Wang (王银珍)[1,*], Pingping Duan (段萍萍)[1], Ning Li (李 宁)[1], Juqing Di (狄聚青)[2,3], Liaolin Zhang (张料林)[4], Junyong Deng (邓俊勇)[4], Xuwei Sun (孙旭炜)[1], Benli Chu (初本莉)[1], and Qinyu He (何琴玉)[1]

[1]*Guangdong Provincial Key Laboratory of Quantum Engineering and Quantum Materials, School of Physics and Telecommunication Engineering, South China Normal University, Guangzhou 510006, China*

[2]*Key Laboratory of Materials for High Power Laser, Shanghai Institute of Optics and Fine Mechanics, Chinese Academy of Sciences, Shanghai 201800, China*

[3]*University of Chinese Academy of Sciences, Beijing 100049, China*

[4]*Institute of Optical Communication Materials and State Key Laboratory of Luminescent Materials and Devices, South China University of Technology, Guangzhou 510640, China*

**Corresponding author: agwyz@aliyun.com*

Received December 27, 2014; accepted March 16, 2015; posted online April 29, 2015

Pr^{3+}/Yb^{3+} co-doped $CaNb_2O_6$ thin films are deposited on Si(100) substrates by pulsed laser deposition and annealed at different temperatures in air atmosphere. X-ray diffraction, Raman spectroscopy, atomic force microscopy, X-ray photoelectron spectroscopy, and photoluminescence spectra are used to characterize the samples. The results show that the annealing temperature has a strong effect on the film's grain size, structure, morphology, and the up-conversion luminescence properties. The grain size and up-conversion luminescence of Pr^{3+}/Yb^{3+} co-doped $CaNb_2O_6$ films increases with the increasing annealing temperature.

OCIS codes: 160.5690, 310.6860.
doi: 10.3788/COL201513.051603.

Rare-earth ion (RE^{3+}) doped up-conversion (UC) luminescence materials have attracted much attention due to their potential applications such as solid-state lasers, light-emitting diodes, high-density storage, display, optoelectronics, medical diagnostics, sensors, and solar energy conversion[1–11]. UC is a luminescence process whereby two or more low-energy photons are converted to one higher-energy photon. Among the lanthanide ions, the Pr^{3+} ion has good luminescence properties and a wide range of applications. Many researchers have studied Pr^{3+} and Yb^{3+} co-doped UC luminescence materials[12–14]. Matrix materials also play an important role in the RE^{3+}-ion-doped UC material. Compared with fluoride and sulfide, matrix material of oxide has great mechanical strength, better physical and chemical stability. $CaNb_2O_6$ has extensive applications in microwave dielectrics[15], photocatalysts[16], lasers[17], laser host materials[18], fibers[19], and cost lamp phosphors[20,21]. However, there are few reports on $CaNb_2O_6$ thin films; optical thin films for integrated devices play an important role in device miniaturization[22].

In this Letter, we report the growth of Pr^{3+}/Yb^{3+} co-doped $CaNb_2O_6$ thin films by pulsed laser deposition (PLD) and investigate the structure and UC luminescence properties of the Pr^{3+}/Yb^{3+} co-doped $CaNb_2O_6$ thin films. To the best of our knowledge, Pr^{3+}/Yb^{3+} co-doped $CaNb_2O_6$ thin films has not been reported previously.

The Pr^{3+}/Yb^{3+} co-doped $CaNb_2O_6$ target was prepared by conventional solid-state reaction methods using analytical grade $CaCO_3$, Nb_2O_5, Pr_6O_{11}, and Yb_2O_3 powders as the starting materials. These powders were weighted according to the molecular formula $Ca_{0.88}Yb_{0.10}Pr_{0.02}Nb_2O_6$. The starting powders were ball-milled for 24 h, then dried and calcinated at 1250 °C for 10 h. The resulting powders were pressed into disk pellets and sintered at 1200 °C for 6 h. The as-prepared target showed a $CaNb_2O_6$ crystalline phase in the X-ray diffraction (XRD) pattern. The Pr^{3+}/Yb^{3+} co-doped $CaNb_2O_6$ thin films were deposited by PLD on Si(100) substrate at room temperature, oxygen pressure of 5.2 Pa, and laser pulse energy power of 300 mJ. Annealing of Pr^{3+}/Yb^{3+} co-doped $CaNb_2O_6$ thin films were carried out for 2 h at temperature of 700, 800, and 900 °C in air. XRD patterns of the samples were done on a Rigaku D/max-IIIA X-ray diffractometer ($Cu-K\alpha 1$, $\lambda = 0.15405$ nm). The surface morphology of Pr^{3+}/Yb^{3+} co-doped $CaNb_2O_6$ thin films were studied by atomic force microscopy (AFM) (Digital Instrument Nanoscope IIIa). The Raman spectrum was taken with excitation of Ar^+ laser at 514.5 nm. X-ray photoelectron spectroscopy (XPS) using an ESCALAB250 system was used to analyze chemical compositions of the films. The UC emission spectra were measured with the laser diode (LD) excitation at the wavelength of 980 nm.

Figure 1 shows the XRD patterns of as-grown and annealed $CaNb_2O_6:Pr^{3+}/Yb^{3+}$ thin films deposited on Si(100) substrates. There is no diffraction peak of as-deposited $CaNb_2O_6:Pr^{3+}/Yb^{3+}$ thin films, indicating that the $CaNb_2O_6:Pr^{3+}/Yb^{3+}$ thin films are amorphous. When the annealing temperature increases to 700 °C, diffraction peaks are clearly observed, indicating the

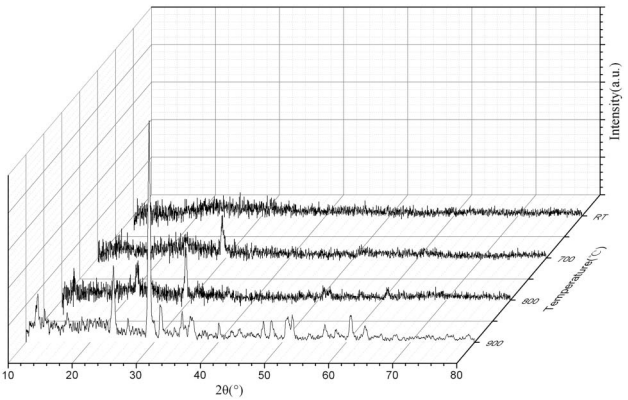

Fig. 1. XRD spectra of as-deposited and annealed films $CaNb_2O_6$:Pr^{3+}/Yb^{3+} films.

polycrystalline phase of $CaNb_2O_6$ thin films with an orthorhombic structure have been developed, which is in agreement with the standard JCPDS card (JCPDS 39–1392). No other peaks or impurities are detected, indicating that these obtained samples are pure $CaNb_2O_6$ thin films and the doping Pr^{3+} and Yb^{3+} do not change the $CaNb_2O_6$ structure. Average crystallite size of crystallized $CaNb_2O_6$ thin films estimated from Scherrer's equation is about 12.5, 15.3, and 21.9 nm for the annealing temperatures of 700, 800, and 900 °C, respectively, the (131) diffraction peak having the highest intensity was selected for the calculation. However, the crystallite size cannot be estimated in the case of the amorphous films due to the absence of diffraction peaks. Full-width half-maximum (FWHM) values for the most intense peak (131) are decreasing after annealing. The increase in crystallite size with annealing temperature may be attributed to the improvement in the crystalline quality, for the annealing provides activation energy to the atoms, allowing them to diffuse and more fully occupy the lattice sites. The $CaNb_2O_6$: Pr^{3+} /Yb^{3+} thin films annealed at 900 °C have comparatively larger crystallite size. These results indicate that the annealing temperature plays an important role in determining the crystallinity.

Figure 2 shows AFM images of the as-deposited and annealed $CaNb_2O_6$:Pr^{3+}/Yb^{3+} thin films. The root-mean square (RMS) roughness values were 1.54, 4.32, 6.94, and 12.16 nm for the as-deposited and annealed $CaNb_2O_6$: Pr^{3+} /Yb^{3+} thin films at 700, 800, and 900 °C, respectively. It can be seen that RMS roughness value increases with the increase of annealing temperature, which is attributed to larger grain size. The increase in surface roughness upon annealing is favorable for solar cells and gas sensor applications.

Figure 3 shows the Raman spectra of the as-deposited and annealed $CaNb_2O_6$: Pr^{3+} /Yb^{3+} films at 900 °C. The Raman spectra present the typical bands corresponding to the normal vibration modes of $CaNb_2O_6$ in the range 100–1000 cm^{-1}[23]. Wavelengths 900, 811, 601, and 430 cm^{-1} are ascribed to Nb–O stretching bands. Wavelength 260 cm^{-1} is ascribed to the O–Nb–O bending

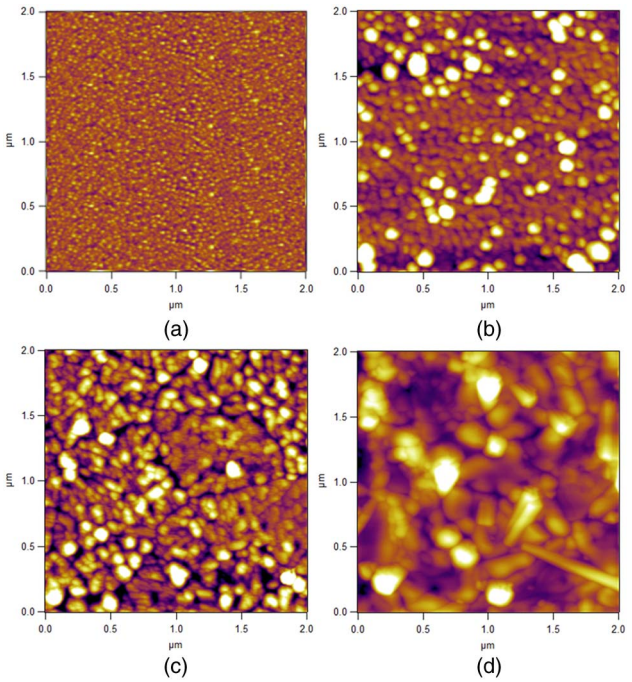

Fig. 2. AFM image of as-deposited and annealed $CaNb_2O_6$: Pr^{3+} /Yb^{3+} thin films; (a) as-deposited; (b) 700 °C; (c) 800 °C; (d) 900 °C.

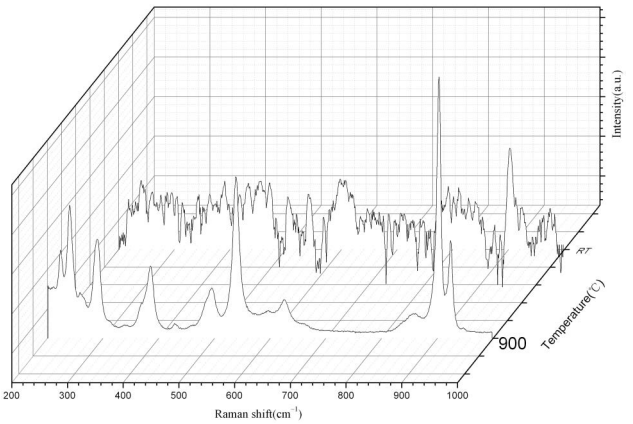

Fig. 3. Raman spectra of as-deposited and annealed $CaNb_2O_6$: Pr^{3+} /Yb^{3+} thin films.

vibration bands. No other peaks were found as in the Raman pattern. The Raman peaks exhibited broadening as-grown compared to 900 °C annealing. The peak broadening and shift of the Raman bands is related to a decrease in particle size and/or degree of order. Increase of annealing temperature does not shift the peak position which depicts the good quality/stability of the films. As annealing temperature increases, the Raman intensities increases and the FWHM of peak decrease. This means that the crystallinity is improved by increasing the annealing temperatures.

Figure 4 shows the XPS spectra in a wide energy range of annealed $CaNb_2O_6$: Pr^{3+} /Yb^{3+} films at 900 °C. The

XPS survey spectrum in Fig. 4 confirms the presence of Ca, O, Nb, Yb, Pr, and C 1 s (from the carbon pollution).

Figure 5 shows UC luminescence spectra of $CaNb_2O_6$: Pr^{3+} /Yb^{3+} thin films under 980 nm excitation at room temperature. It can be seen that the UC emission is composed mainly of the red $^1D_2 \rightarrow {}^3H_4$ emission at 610 nm and weak emission centered around 532, 562, and 654 nm corresponding to the $^3P_1 \rightarrow {}^3H_5$, $^3P_0 \rightarrow {}^3H_5$, and $^3P_0 \rightarrow {}^3F_2$ transitions of Pr^{3+} ions, respectively. Pumping of the Pr^{3+} excited-state emitting levels is accomplished through a combination of multiphonon-assisted absorption of the Yb^{3+} sensitizer. The intensity of the UC emission spectra increases with the increase of annealing temperature due to improved crystallinity, the improved crystallinity can help to reduce the defects of films, which may well lead to the reduction of quenching centers and the increase of the luminescence intensity[24,25].

To understand the UC emission mechanism in the $CaNb_2O_6$: Pr^{3+} /Yb^{3+} thin films, the dependence of UC emission intensities on the pump power is shown in Fig. 6, It is known that the number of photon is required to populate the upper emission state that can be obtained by the following equation: $I_{UC} \propto P^n$, where I_{UC} is the fluorescent intensity, P is the pump laser power, and n is the number of photons needed to produce the fluorescence[26]. As shown in Fig. 6, the slope n values for $^3P_0 \rightarrow {}^3H_5$, $^1D_2 \rightarrow {}^3H_4$, and $^3P_0 \rightarrow {}^3F_2$ are 2.15, 1.96, and 2.23, respectively, indicating two-photon processes under 980 nm excitation. Figure 7 shows energy level diagram of $CaNb_2O_6$: Pr^{3+} /Yb^{3+} thin films and UC emission processes under 980 nm excitation. In the Pr^{3+} /Yb^{3+} co-doped $CaNb_2O_6$ thin films, the Yb^{3+} ion acts as sensitizers to absorb 980 nm excitation light from $^2F_{7/2}$ ground-state to the $^2F_{5/2}$ excitation state. The excited Yb^{3+} ion transfers its energy to neighbor Pr^{3+} ion in the $^3H_4$ ground-state, exciting it to the $^1G_4$ level. Subsequently, Pr^{3+} ion can be further excited to $^3P_0$ upper emitting level after absorption of a second laser photon. Finally, the

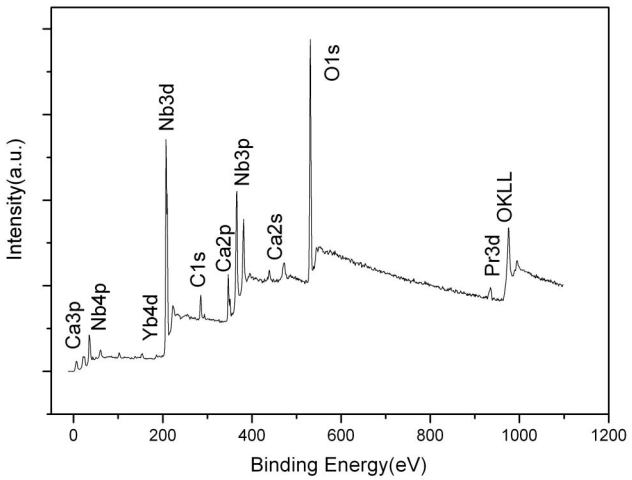

Fig. 4. XPS spectra of $CaNb_2O_6$: Pr^{3+} /Yb^{3+} films.

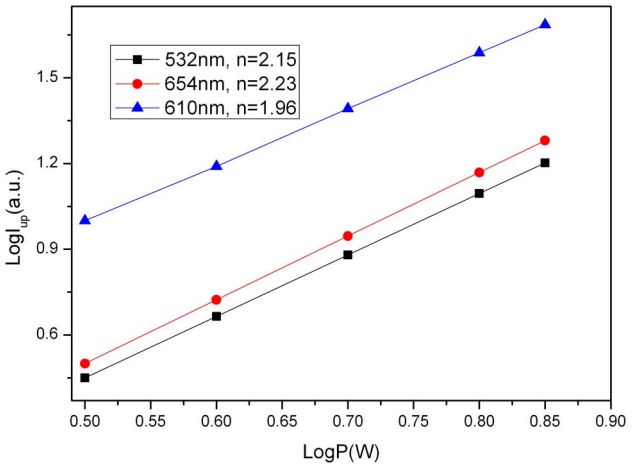

Fig. 6. Variation of UC emission intensities with pump power.

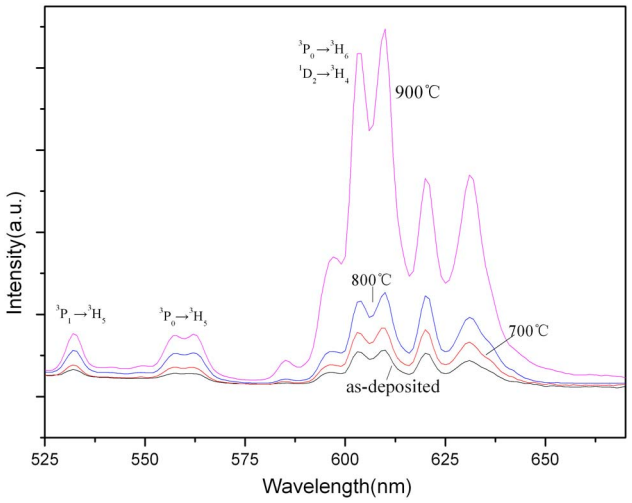

Fig. 5. UC emission spectra of as-deposited and annealed $CaNb_2O_6$: Pr^{3+} /Yb^{3+} thin films under 980 nm LD excitation.

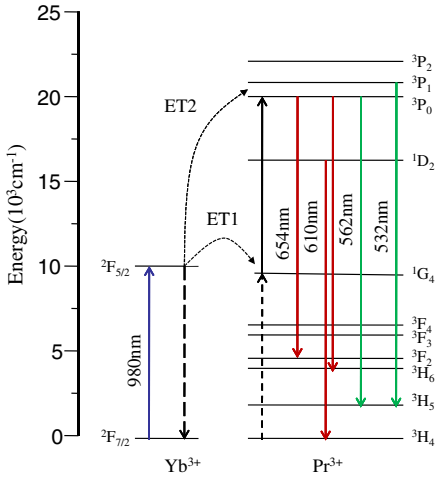

Fig. 7. Energy level diagram and a possible mechanism in $CaNb_2O_6$:Pr^{3+}/Yb^{3+} thin films under 980 nm LD excitation.

excited Pr^{3+} ion in $^3P_0$ level radiatively demotes to the $^3H_5$, $^3H_6$, and $^3F_2$ states to generate the visible fluorescence emission bands at 532, 562, 610, and 654 nm.

In conclusion, the Pr^{3+}/Yb^{3+} co-doped $CaNb_2O_6$ films are prepared on Si(100) substrates by PLD and are characterized by XRD, AFM, Raman, XPS, and UC luminescence measurements. The results show that the UC emission intensity of Pr^{3+}/Yb^{3+} co-doped $CaNb_2O_6$ films increases with increasing annealing temperature. Under 980 nm excitation, emission bands at 532, 562, 610, and 654 nm of Pr^{3+} are observed, UC emission is a two-photon absorption process.

This work was supported by the National Natural Science Foundation of China (Nos. 11474104 and 51372092) and the China Postdoctoral Science Foundation (No. 2012M511801).

References

1. G. Huber, ECS Trans. **25**, 287 (2009).
2. N. C. Bigall, W. J. Parak, and D. Dorfs, Nano Today **7**, 282 (2012).
3. X. Hou, S. Zhou, T. Jia, H. Lin, and H. Teng, J. Alloys Comp. **509**, 2793 (2011).
4. H. X. Zhang, C. H. Kam, Y. Zhou, X. Q. Han, S. Buddhudu, Q. Xiang, Y. L. Lam, and Y. C. Chan, Appl. Phys. Lett. **77**, 609 (2000).
5. B. M. Van der Ende, L. Aarts, and A. Meijerink, Phys. Chem. Chem. Phys. **11**, 11081 (2009).
6. R. Scheps, Prog. Quant. Electron. **20**, 271 (1996).
7. K. Teshima, S. Lee, N. Shikine, T. Wakabayashi, K. Yubuta, T. Shishido, and S. Oishi, Cryst. Growth Des. **11**, 995 (2011).
8. A. Fang, Z. Dai, T. Luo, G. Sun, L. Wang, and Z. Jiang, Chin. Opt. Lett. **3**, 164 (2005).
9. D. Yan, Z. Yang, Ji. Liao, H. Wu, J. Qiu, Z. Song, D. Zhou, Y. Yang, and Z. Ying, Chin. Opt. Lett. **11**, 041602 (2013).
10. J. Zhou, N. Shirahata, H. Sun, B. Ghosh, M. Ogawara, Y. Teng, S. Zhou, R. G. S. Chu, M. Fujii, and J. Qiu, J. Phys. Chem. Lett. **4**, 402 (2013).
11. X. Shang, P. Chen, W. Cheng, K. Zhou, J. Ma, D. Feng, S. Zhang, Z. Sun, J. Qiu, and T. Jia, J. Appl. Phys. **116**, 063101 (2014).
12. J. Di, X. Xu, C. Xia, D. Li, D. Zhou, Q. Sai, L. Wang, and J. Xu, Physica B: Condens. Matter **408**, 1 (2013).
13. A. Pandey and V. K. Rai, Mater. Res. Bull. **57**, 156 (2014).
14. Y. Yang, F. Jiao, W. Zhang, J. Jiao, Z. Li, X. Su, and N. Wen, J. Alloys Comp. **567**, 107 (2014).
15. R. C. Pullar, J. D. Breeze, and N. M. Alford, J. Am. Ceram. Soc. **88**, 2466 (2005).
16. I. S. Cho, S. T. Bae, D. K. Yim, D. W. Kim, and K. S. Hong, J. Am. Ceram. Soc. **92**, 506 (2009).
17. A. A. Ballman, S. P. S. Porto, and A. Yariv, J. Appl. Phys. **34**, 3155 (1963).
18. D. Z. Li, X. D. Xu, C. W. Xu, J. Zhang, D. Y. Tang, Y. Cheng, and J. Xu, Opt. Lett. **36**, 3888 (2011).
19. A. S. S. Decamargo, R. A. Silva, J. P. Andreeta, and L. A. O. Nunes, Appl. Phys. B **80**, 497 (2005).
20. D. van der Voort, J. M. E. de Rijk, and G. Blasse, Physica Status Solidi A **135**, 621 (1993).
21. R. Zhou, X. Wei, C. Duan, Y. Chen, and M. Yin, ECS J. Solid State Sci. Technol. **1**, R147 (2012).
22. H. Chen, B. Yang, Y. Sun, M. Zhang, Y. Sui, Z. Zhang, and W. Cao, J. Lumin. **131**, 2574 (2011).
23. E. Husson, Y. Repelin, N. Q. Dao, and H. Brusset, Spectrochim. Acta A **33**, 995 (1977).
24. M. Bailly, G. Costentin, H. Lauron-Pernot, J. M. Krafft, and M. Che, J. Phys. Chem. B **109**, 2404 (2005).
25. J. H. Jeong, J. S. Bae, S. S. Yi, J. C. Park, and Y. S. Kim, J. Phys. Condens. Matter **15**, 567 (2003).
26. E. De la Rosa, P. Salas, H. Desirena, C. Angeles, and R. A. Rodríguez, Appl. Phys. Lett. **87**, 241912 (2005).